Osteoarthritis and Cartilage 27 (2019) 1692–1701

Osteoarthritis and Cartilage

Protective effects of extracorporeal shockwave on rat chondrocytes and temporomandibular joint osteoarthritis; preclinical evaluation with *in vivo* ^{99m}Tc-HDP SPECT and *ex vivo* micro-CT

Y.-H. Kim † [a], J.-I. Bang † [a], H.-J. Son †, Y. Kim ‡, J.H. Kim §, H. Bae ‖, S.J. Han ‖, H.-J. Yoon † [* b], B.S. Kim † [** b]

† *Department of Nuclear Medicine, Ewha Womans University School of Medicine, Seoul, South Korea*
‡ *Department of Conservative Dentistry, Ewha Womans University School of Medicine, Seoul, South Korea*
§ *Department of Oral Health Science, Ewha Womans University Graduate School of Clinical Dentistry, Seoul, South Korea*
‖ *Department of Rehabilitation Medicine, Ewha Womans University School of Medicine, Seoul, South Korea*

ARTICLE INFO

Article history:
Received 27 March 2019
Accepted 6 July 2019

Keywords:
Temporomandibular joint osteoarthritis
Extracorporeal shock wave
Chondrocytes
Technetium 99m hydroxyethylene-diphosphonate
Single photon emission computed tomography
Micro CT

SUMMARY

Objective: Extracorporeal shockwave therapy (ESWT) has been shown to have chondroprotective effects on arthritic diseases. We investigated the effects of ESWT on temporomandibular joint osteoarthritis (TMJOA) using rat chondrocytes and TMJOA rat models.

Design: Cell viability and expression of pro-inflammatory cytokines, cartilage degradation, and apoptosis markers were measured in control, monosodium iodoacetate (MIA)-treated and ESWT plus MIA-treated chondrocytes *in vitro*, and intra-articular MIA injection (TMJOA) and ESWT on TMJOA rats *in vivo*. *In vivo* ^{99m}Tc-hydroxymethylene diphosphonate (HDP) single-photon emission computerized tomography/computerized tomography (SPECT/CT) and *ex-vivo* micro-CT and histologic examinations were performed in rat models.

Results: ESWT plus MIA-treated chondrocytes showed increased cell viability significantly ($P = 0.007$), while decreased genetic expression of pro-inflammatory cytokines [tumor necrosis factor-α (TNF-α), interleukin-1β (IL-1β), and interleukin-6 (IL-6); $P < 0.001$ for each] and cartilage degradation markers [matrix metalloproteinase-3 (MMP3), matrix metalloproteinase-13 (MMP13), and bone morphogenetic protein 7 (BMP7); $P < 0.001$ for each], and number of apoptotic cells ($P < 0.001$) compared to MIA-treated chondrocytes. Changes in cytochrome c and cleaved caspase-3 levels relative to procaspase-3 were decreased over MIA-treated chondrocytes. ESWT on TMJOA rat models was associated with a significant decrease in pro-inflammatory and cartilage degradation markers, as demonstrated by real-time PCR and immunohistochemistry stains ($P < 0.001$ for each). On ^{99m}Tc-HDP SPECT/CT, the ESWT group showed a significantly lower uptake ratio compared to the TMJOA group ($P = 0.008$). Micro-CT analysis revealed that the ESWT group showed improved structure and bone quality compared to the TMJOA control group.

Conclusions: ESWT was associated with a protective effect on cartilage and subchondral bone structures of TMJOA by reducing inflammation, cartilage degradation, and chondrocyte apoptosis.

* Address correspondence and reprint requests to: H.-J. Yoon, Department of Nuclear Medicine, Ewha Womans University School of Medicine, 911-1 Mok-Dong, Yangchun-Ku, Seoul 158-710, South Korea. Tel: 82-2-2650-2053; Fax: 82-2-2650-2063.
** Address correspondence and reprint requests to: B.S. Kim, Department of Nuclear Medicine, Ewha Womans University School of Medicine, 911-1 Mok-Dong, Yangchun-Ku, Seoul 158-710, South Korea. Tel: 82-2-6986-1725; Fax: 82-2-2650-2063.
E-mail addresses: cine82@hanmail.net (Y.-H. Kim), bangjiin@gmail.com (J.-I. Bang), sshj3534@nate.com (H.-J. Son), yemis@ewha.ac.kr (Y. Kim), jihoi3537@gmail.com (J.H. Kim), acebhs@ewha.ac.kr (H. Bae), ocrystal@ewha.ac.kr (S.J. Han), haijeon.yoon@gmail.com (H.-J. Yoon), kbomsahn@ewha.ac.kr (B.S. Kim).
[a] Y.-H. Kim and J.-I. Bang evenly contributed to this work.
[b] H.-J. Yoon and B.S. Kim evenly contributed to this work.

https://doi.org/10.1016/j.joca.2019.07.008
1063-4584/

Introduction

Temporomandibular joint osteoarthritis (TMJOA) is a common osteoarthritic problem affecting approximately 15% of the population, and a leading subtype of temporomandibular disorders[1]. TMJOA can cause severe pain and dysfunction and diminish quality of life. Unlike osteoarthritis (OA) in the knee or hip, the pathogenesis of TMJOA remains unclear, with interactions of multifactorial etiologies having been proposed[2,3]. Along with mechanical stress, inflammation and chondrocyte apoptosis have been recognized as important in the pathogenesis of TMJOA[4–6].

Traditional treatments of TMJOA are mainly nonsurgical interventions and multimodal strategies. These treatment approaches remain largely symptomatic, including habit modification, oral appliance therapy, physical therapy, pulsed electrical stimulation, oral drugs for suppressing inflammation or reducing pain, topical/intraarticular agents, and supplements[2,3,7]. Although there remain controversies about these treatment choices, we propose that the therapeutic aim for TMJOA be pointed towards suppressing inflammatory processes to prevent joint deformities and preserve joint function.

Extracorporeal shock wave therapy (ESWT) has been widely used in different musculoskeletal diseases[8,9]. Although the biochemical mechanisms of ESWT are not fully understood, many lines of evidence have indicated that ESWT could induce anti-inflammatory action that promotes the healing and regeneration of tissue[10,11]. A previous study reported that ESWT could prevent histological destruction in knee joints by reducing inflammation and chondrocyte apoptosis[12]. In addition to knee joints, other joints and orthopedic problems have been targeted for ESWT application.

Although attempt to apply ESWT to TMJ disorders has been reported[13], the therapeutic effects of ESWT on TMJOA have yet to be thoroughly investigated. We hypothesized that ESWT could reduce inflammation, cartilage degradation, and apoptosis in TMJOA. We performed an *in vitro* evaluation using rat-derived chondrocytes, and an *in vivo* animal study using TMJOA rat models to explore how ESWT alters the microenvironment in TMJOA. In addition, we evaluated the capacity of *in vivo* ^{99m}Tc-hydroxymethylene diphosphonate (HDP) bone single-photon emission computerized tomography/computerized tomography (SPECT/CT) and *ex vivo* micro-CT imaging in the analysis of the TMJOA microenvironment.

Materials and methods

All experimental procedures were approved by the Institutional Animal Care and Use Committee of Ewha Womans University.

Preparation of primary rat chondrocytes

Primary rat chondrocytes were isolated as previously described[14]. Briefly, cartilage from femoral heads was harvested from 4-week-old male Sprague–Dawley rats. Cartilage samples were digested with trypsin–ethylenediaminetetraacetic acid (EDTA) and 0.2% Collagenase II (Sigma–Aldrich) for 15 min and 3 h, respectively. Then, chondrocytes were cultured in Minimum essential Eagle's medium (MEM; Sigma–Aldrich) at 37°C in 5% CO_2. For all experiments, early passage cells (primary to 3) were used.

Monosodium iodoacetate (MIA; Sigma–Aldrich) induces cartilage degradation and loss through the inhibition of glyceraldehyde-3-phosphate dehydrogenase[14]. Chondrocytes were exposed to MIA for 24 h to test MIA-induced inhibition therein (MIA group). Chondrocytes were treated using Dornier AR2 electromagnetic head applicator equipped with smart focus technology, and then concomitantly treated with MIA for 24 h to investigate the protective effects of ESWT on MIA-treated chondrocytes (ESWT + MIA group). For ESWT, cells were harvested and suspended in tubes completely filled with culture medium. Each tube was placed in vertical alignment with the head applicator and was adjusted so that the central point of the applicator corresponded to the center of the bottom of the tube. The tube was kept in contact with the applicator unit by means of a water-filled cushion while remaining in the focal area of the shock wave source[15]. The distance between the probe and the chondrocyte layer on the tube bottom was maintained at 10 mm (Fig. 1).

Cell proliferation assay

We performed a 3-(4,5-dimethylthiazol-2-yl)-2,5-diphenyltetrazolium bromide (MTT) assay (Sigma–Aldrich) to set the optimal concentration of MIA for rat chondrocytes[16]. Briefly, chondrocytes were plated in a 96-well microtiter plate at a density of 2×10^4 cells per well in a final volume of 200 mL MEM. Cells were treated with stepped concentrations of MIA (0.5, 1.5, 3.0, 6.0, 12.0, 24.0, and 48.0 μM, or no MIA for control) for 24 h. After treatment, cells were incubated in an MTT solution (0.5 mg/mL) for 3 h at 37°C. Formazan crystal formations of were dissolved in dimethyl sulfoxide (DMSO) (Sigma–Aldrich) at room temperature (RT) in the dark for 1 h, and absorbances were read at 570 nm on a VersaMax microplate reader (Molecular Devices).

An MTT assay was performed after ESW treatment on rat chondrocytes to determine the optimal level of ESWT for chondrocyte proliferation. Chondrocytes were treated with 500 shots of ESW (0.025, 0.068, 0.124, 0.166, 0.214, and 0.272 mJ/mm^2). Then, an MTT assay was performed according to the procedure described above.

In vitro real-time polymerase chain reaction (PCR) analysis

Real-time PCR was performed to assess gene expression levels related to pro-inflammatory cytokines, cartilage degradation markers such as matrix metalloproteinases (MMPs), and bone morphogenetic protein (BMP) in chondrocytes. Chondrocytes (2×10^5 cells) were exposed to MIA for 24 h in the presence or absence of ESWT. Total RNA was extracted from cells using a MiniBEST Universal RNA Extraction Kit (Takara) and converted into complementary DNA using a PrimeScript™ RT Master Mix (Takara). The primers for tumor necrosis factor-α (TNF-α), interleukin-1β (IL-1β), IL-6, MMP3, MMP13, and BMP7 are shown in Table I. Real-time PCR was performed with a toluidine blue (TB) Green™ Fast qPCR Mix (Takara) on a QuantStudio 3 Real-Time PCR System (Applied Biosystems) instrument with the following parameters: 95°C for 30 s, 40 cycles of 95°C for 10 s, and 60°C for 30 s. Relative expression levels were normalized to glyceraldehyde 3-phosphate dehydrogenase (GAPDH) expression.

In vitro Western blot analysis

Chondrocytes (2×10^6 cells) were exposed to MIA for 24 h in the presence or absence of ESWT. Using a Mitochondria Isolation Kit for Cultured Cells, mitochondria were separated from the cytosol. Total protein was isolated from cells using PRO-PREP™ Protein Extraction Solution (iNtRON Biotech). The lysates of the samples were separated by sodium dodecyl sulfate polyacrylamide gel electrophoresis (SDS-PAGE) and transferred to polyvinylidene difluoride (PVDF) membranes (Bio-Rad Laboratories). The membranes were subsequently blocked with 5% skim milk for 1 h at RT and incubated overnight at 4°C with primary antibodies targeting cytochrome c (Cell Signaling Technology; diluted 1:500), procaspase and cleaved caspase-3 (Cell Signaling Technology; diluted 1:500) and β-actin (Santa Cruz Biotechnology; diluted 1:1000). Membranes were then

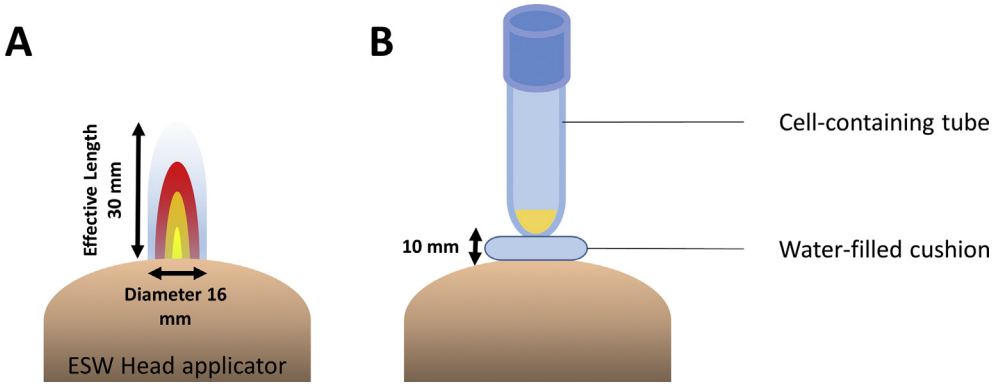

Fig. 1. Schematic figure of ESW treatment. (A) Effective length of the shock wave from the center of the head applicator was 30 mm, and the diameter of the focal zone was 16 mm at an energy flux density of 0.068 mJ/mm^2. (B) During *in vitro* ESW administration, the bottom of the sample tube was placed inside the focal zone, and the distance between the applicator and the chondrocyte layer on the bottom was maintained at 10 mm.

Table I
Primer sequences used for real-time, reverse-transcriptase PCR

Genes	Forward	Reverse	Size (bp)
GAPDH	GGCACAGTCAAGGCTGAGAATG	ATGGTGGTGAAGACGCCAGTA	143
TNF-α	AACTCGAGTGACAAGCCCGTAG	GTACCACCAGTTGGTTGTCTTTGA	133
IL-1β	CTTCGTTAAATGACCTGCAGCTTG	AGGTCGGTCTCACTACCTGTGATG	199
IL-6	CCACTTCACAAGTCGGAGGCTTA	GTGCATCATCGCTGTTCATACAATC	108
MMP3	ACCTATTCCTGGTTGCTG	GGTCTGTGGAGGACTTGTA	105
MMP13	CTGACCTGGGATTTCCAAAA	ACACGTGGTTCCCTGAGAAG	96
BMP-7	ATCCCCAATGTCTCACCACCTA	AAGTATGCTGCTTATCAACCACG	156

TNF-α: tumor necrosis factor-α; IL-1β: interleukin-1β; IL-6: interleukin-6; MMP3: matrix metalloproteinase-3; MMP13: matrix metalloproteinase-13; BMP-7: bone morphogenetic protein 7.

probed with HRP-conjugated anti-rabbit or anti-mouse IgG (Cell Signaling Technology). Signal intensities were measured with an LAS-3000 imaging system (Fujifilm). The relative intensities of cytochrome c, procaspase-3, cleaved caspase-3, and β-actin are presented in the Results section.

Analysis of apoptosis by flow cytometry

Changes in chondrocyte apoptosis were quantified with flow cytometry by loading FITC–annexin V (A5)/propidium iodide (PI, BD Biosciences) double-fluorescence labeling. Following treatment with MIA in the presence or absence of ESWT, cells (1×10^5 cells/100 μL) were collected by centrifugation and incubated in buffer containing FITC–A5 and PI. Apoptotic cells were measured by flow cytometry (ACEA Biosciences). The flow cytometric data were analyzed using NovoExpress software (ACEA Biosciences).

Induction of the TMJOA rat model and ESWT application

Specific pathogen-free (SPF) male Sprague–Dawley rats (200–230 g, 7 weeks old, Orient Bio) were acclimated for 1 week, and then randomly assigned to three groups; a control group ($n = 6$), a TMJOA group ($n = 9$), and an ESWT group ($n = 12$). The TMJOA model was induced by injection of 1 mg MIA dissolved in 50 μL saline into the upper compartment of the right TMJ with a 27-gauge, 0.5-inch needle as described previously[17]. ESW treatment was started 3 days after the MIA injection, and then regularly administered under anesthesia with isoflurane every 3 days for 2 weeks for a total of four administrations. Briefly, the ESW applicator was gently placed on the right TMJ by means of a gel and treated with 500 shocks (energy level = 0.068 mJ/mm^2; frequency = 5 pulses/s).

Ex vivo real-time PCR analysis

Rats were sacrificed via CO_2 inhalation 4 weeks after MIA injection. Condylar heads from the mandibles were isolated, and soft tissues were carefully removed. Total RNA was extracted from the condylar heads. Primers for TNF-α, IL-1β, IL-6, MMP3, MMP13, and caspase-3 were used. All experiments used the same *in vitro* real-time PCR method.

Histopathology and immunostaining

Condylar heads were amputated and fixed in 4% paraformaldehyde for 7 days at 4°C. Bone tissue was decalcified for about 3 weeks at 4°C in a solution with 14% EDTA (pH 7.2, Sigma–Aldrich). After decalcification, condylar heads were washed and prepared for paraffin embedding. Sagittal sections (5 μm) from the center of the head were used for staining with hematoxylin and eosin (H&E) for routine histological evaluation. Safranin O/fast green (SO) and TB stains were used to evaluate proteoglycans in the cartilage matrix[18]. Cartilage thickness was measured five times in SO-stained images, and percentage of cartilage area was measured three times in TB-stained images using ImageJ software (NIH, Bethesda, USA) as described previously[19].

Immunohistochemical (IHC) staining was performed for caspase-3 (Cell Signaling Technology), TNF-α (Abcam), and MMP-3 (Santa Cruz Biotechnology) to assess apoptosis, inflammation, and remodeling in bones and joints. We demonstrated immunoreactivity using a VECTASTAIN ABC Kit (Vector Laboratories). We identified immuno-activity using five frames from the same specimen with a digital microscope camera (Olympus Corporation). Images were analyzed with Image-Pro Plus image analysis software (Media Cybernetics). For quantitative measurements, percentages refer to the sum of the positively stained cells divided by the total

sum of cells counted on all five frames; the average was chosen as the result. Two independent evaluators who were blinded to the nature of the study performed the measurements on all specimens.

In vivo ^{99m}Tc-HDP SPECT/CT imaging analysis

Rats (control, $n = 3$; TMJOA, $n = 6$; ESWT, $n = 6$) were anesthetized with 2% isoflurane and intravenously injected with ^{99m}Tc-HDP (80.9 ± 7.0 MBq) 4 weeks after MIA injection. At 3 h post-injection, rats were placed supine (ventrodorsally) on the bed of a dedicated small animal SPECT/CT scanner (NanoSPECT/CT, Bioscan). A high-resolution static scan of the head region was acquired in helical scanning mode of 180 projections over a 20 min period using a four-head scanner with 4 × 9 (1.4 mm) pinhole collimators with a 140 keV ± 15% energy window. Then, CT images were obtained with the X-ray source set at 45 kVp and 177 μA. The SPECT images were reconstructed to produce an image size of 176 × 176 × 136 voxels with a voxel size of 0.2 × 0.2 × 0.2 mm. CT images had 48 μm resolution acquisition with a voxel-pixel size of 0.20:0.192 mm[20]. We measured uptake ratios of TMJ using the lateral skulls as the background according to the following equation: TMJ uptake ratio = (TMJ counts)/(BG counts). For the measurement of counts, isocontour regions of interest (ROIs) with a 50% threshold were placed over the TMJ and lateral skulls, respectively, using P-mode software (PMOD Technologies).

Ex vivo micro-CT imaging analysis

Rats were sacrificed via CO_2 inhalation (control, $n = 3$; TMJOA, $n = 3$; ESWT $n = 6$) 4 weeks after MIA injection, and mandibles were dissected and fixed in 4% paraformaldehyde. A micro CT system (Skyscan 1173, Bruker) was used to perform 2D and 3D morphometry. The parameters used were in accordance with the guide for evaluation of bone microarchitecture in rodents using micro-computed tomography[21]. Specimens were scanned at a 9.94 μm resolution with an exposure time of 500 msec, an electric voltage of 110 kV, and a current of 72 μA adjusted to allow for maximum differentiation between mineralized and non-mineralized tissues, and a 0.1 mm-thick aluminum filter.

After ROI standardization, images were converted to grayscale using a scale ranging from 0 to 255, with a minimum value of 70 and a maximum value of 100 in all groups. These values were determined based on visualization of the cancellous bone structure located in the ROI. Bone volume density, which describes the ratio of segmented bone volume to total volume (BV/TV), three-dimensional trabecular number (Tb.N), trabecular separation (Tb.S), and closed porosity (%, Po(cl)), open porosity (%, Po(op)), and total porosity (%, Po(tot)) were extracted and analyzed[22].

Statistics

Statistical analyses were performed using MedCalc software (version 12). All data were presented as median with interquartile range (IQR). The differences among different groups were tested with the Kruskal–Wallis test, and an adjusted *P* value via *post hoc* Bonferroni test for multiple comparisons was shown. All tests were two-sided, and a *P*-value less than 0.05 was considered statistically significant.

Results

In vitro effects of ESWT on MIA-treated chondrocytes

The optimal concentration of MIA was set to 3.0 μM in accordance with the results of the MTT assay that showed a sharp drop in cell viabilities at 3.0 μM of MIA that was sustained up to 48.0 μM of MIA [Supplementary Fig. 1(A)]. The level of energy of ESW treatments showed no demonstrable adverse effects on cell viabilities of rat chondrocytes, and 0.068 mJ/mm^2 was selected for subsequent experiments [Supplementary Fig. 1(B)].

Rat chondrocytes showed a significant decrease in cell viability after MIA treatment, and this reduced viability was significantly recovered upon ESW treatment [$P < 0.001$ and $P = 0.007$, respectively; Fig. 2(A)].

Significant increases in gene expression levels of TNF-α, IL-1β, IL-6, MMP3, MMP13, and BMP7 were shown after 24 h of MIA treatment in rat chondrocytes. With ESW treatment, all up-regulated gene transcripts were significantly decreased [$P < 0.001$ for each; Fig. 2(B)].

Results of the Western blot are shown in Fig. 2(C). Chondrocytes in control cultures constitutively expressed cytochrome c, procaspase-3, and cleaved caspase-3 apoptosis markers. After 24 h of MIA treatment, the ratio of cytosolic cytochrome c and cleaved caspase-3 to procaspase-3 increased 2.6-fold and 8.8-fold, respectively, over control. With ESW treatment, the ratio of protein levels of cytochrome c and cleaved caspase-3 to procaspase-3 decreased 0.6-fold and 0.8-fold, respectively, compared the 24 h MIA-treated chondrocytes without ESWT [Fig. 2(D)].

The 24 h MIA treatment resulted in a significant increase in the number of early and late stage apoptotic cells compared to control ($P = 0.001$ and $P = 0.002$, respectively). ESW treatment was associated with a significant attenuation of MIA-induced apoptosis in chondrocytes [$P < 0.001$ and $P < 0.001$; Fig. 2(E) and (F)].

In vivo effects of ESWT on TMJOA rat model

The experimental schedule is illustrated briefly in Fig. 3. Chondrocytes were isolated from condylar cartilage for all groups. Significant increases in gene expression levels of TNF-α, IL-1β, IL-6, MMP3, MMP13, and caspase-3 were shown in the TMJOA group. All up-regulated gene transcripts were significantly reduced in the ESWT group [$P < 0.001$ for each; Fig. 4(A)].

Condyle cartilage structure was observed by H&E, SO, and TB stains in the control and experimental groups. A significant decrease in cartilage thickness and percentage of area of proteoglycans in the condylar cartilage was found for the TMJOA group ($P = 0.005$ and $P < 0.001$, respectively), and recovered to levels similar to the control group after ESW treatment [$P < 0.001$; Fig. 4(B) and (C)].

The TMJOA group experienced significantly higher expression levels of caspase-3, TNF-α, and MMP3 than the control group ($P < 0.001$ for each). Chondrocytes positive for caspase-3, TNF-α, and MMP3 decreased significantly in the ESWT group compared to the TMJOA group [$P < 0.001$ for each; Fig. 4(D) and (E)].

^{99m}Tc-HDP SPECT/CT and micro-CT analysis

In vivo joint uptake of ^{99m}Tc-HDP in TMJ was evaluated using SPECT/CT for small animals and compared among groups (Fig. 5). The TMJOA group showed significantly higher TMJ uptake ratios than the control group ($P = 0.002$). The ESWT group showed significantly lower TMJ uptake ratios compared to the TMJOA group ($P = 0.008$).

Changes in the microarchitecture of TMJ subchondral bone were evaluated by micro-CT and compared among groups. The TMJOA group showed a trend toward lower bone volume densities (BV/TV; $P = 0.079$) and significantly lower Tb.N values ($P = 0.006$) compared to the control group, but significantly higher values for both than the ESWT group ($P = 0.038$). Tb.S values were significantly higher in the TMJOA group than in the control group

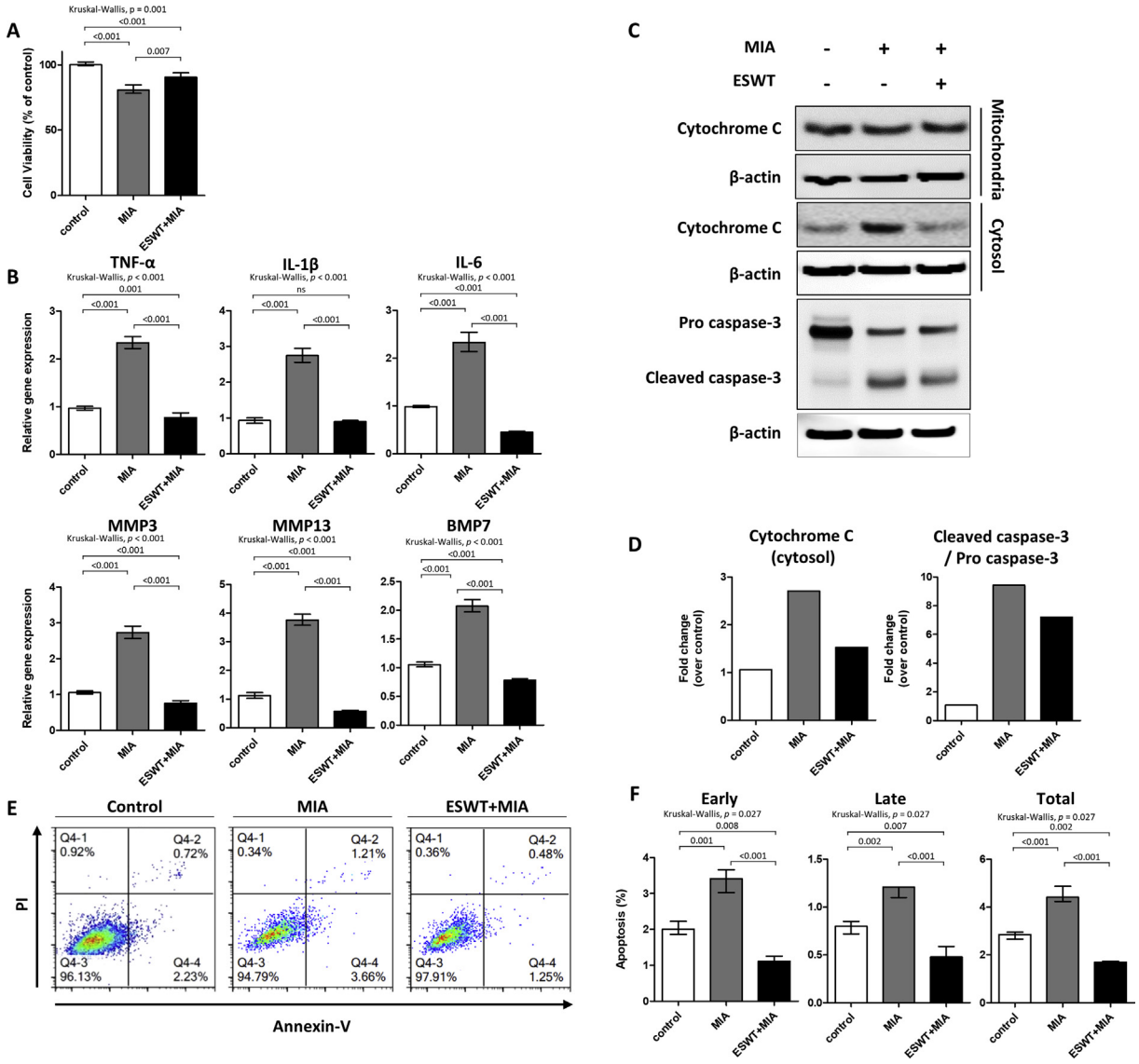

Fig. 2. ***In vitro*** **effects of ESWT on MIA-treated chondrocytes.** Results from MTT, PCR, Western blot, and flow cytometry assays on the effects of ESWT (0.068 mJ/mm^2, 5 pulses/s) on MIA (3.0 μM, 24 h)-treated chondrocytes. All experiments were performed in triplicate for each condition and repeated at least twice. (A) MTT assay for cell viability of chondrocytes after MIA and ESW treatment; chondrocytes (control), chondrocytes with MIA (MIA), and ESW-treated chondrocytes with MIA (ESWT + MIA). (B) Real time-PCR gene expression analysis of pro-inflammatory cytokines (TNF-α, IL-1β, IL-6), and cartilage degradation markers (MMP3, MMP13, and BMP7) on rat chondrocytes. (C–D) Western blot analysis on rat chondrocytes after MIA and ESW treatment. Protein levels of cytochrome c, procaspase-3, and cleaved caspase-3 were analyzed as apoptosis markers. (E, F) Apoptosis analysis of rat chondrocytes after MIA and ESW treatments. Apoptosis was measured by an A5 and PI dual staining assay, followed by fluorescence-activated cell sorting (FACS) analysis. Q4-4: A5 immunoreactive cells; Q4-1: PI immunoreactive cells; Q4-2: A5 and PI immunoreactive cells. The percentages of A5-and PI-positive cells are shown as early and late apoptosis markers, respectively. Values are presented as median with IQR.

($P = 0.009$) and significantly lower in the ESWT group than in the TMJOA group ($P = 0.016$). The TMJOA group showed significantly higher Po(tot) and Po(op) ($P < 0.05$ for each) than in the control or ESWT groups, while Po(cl) was significantly lower than in the ESWT group [$P = 0.032$; Fig. 6].

Discussion

In this study, ESWT significantly reduced the expression of pro-inflammatory cytokines, cartilage degradation, and chondrocyte apoptosis induced by MIA on rat chondrocyte and rat TMJ cartilage. The results of this study indicated that the application of ESWT might yield protective effects on the cartilage of MIA-induced TMJOA of in rats.

Pathogenesis of TMJOA has been focused on inflammation-induced deterioration of cartilage. Pro-inflammatory cytokines such as IL-1β, IL-6, and TNF-α are increased in the synovial fluid of patients with TMJOA[4,23]. Apoptosis of chondrocytes causes cartilage degradation and may contribute to the destruction of subchondral bones[3]. Although the pathogenesis of TMJOA has yet to be fully delineated, anti-inflammation should be a goal for TMJOA therapy. Previously, targeting of inflammatory process using cyclooxygenase (COX)-2 inhibitors was associated with the down-regulation of IL-1β and MMPs, with protective effects on the extracellular matrix metabolism of mandibular chondrocytes affected by mechanical stress[24]. Attempts to repair TMJ using tissue regeneration via chondrogenic stem cells was also tried[25]. Also, low intensity pulsed ultrasound (LIPUS) has recently shown possible

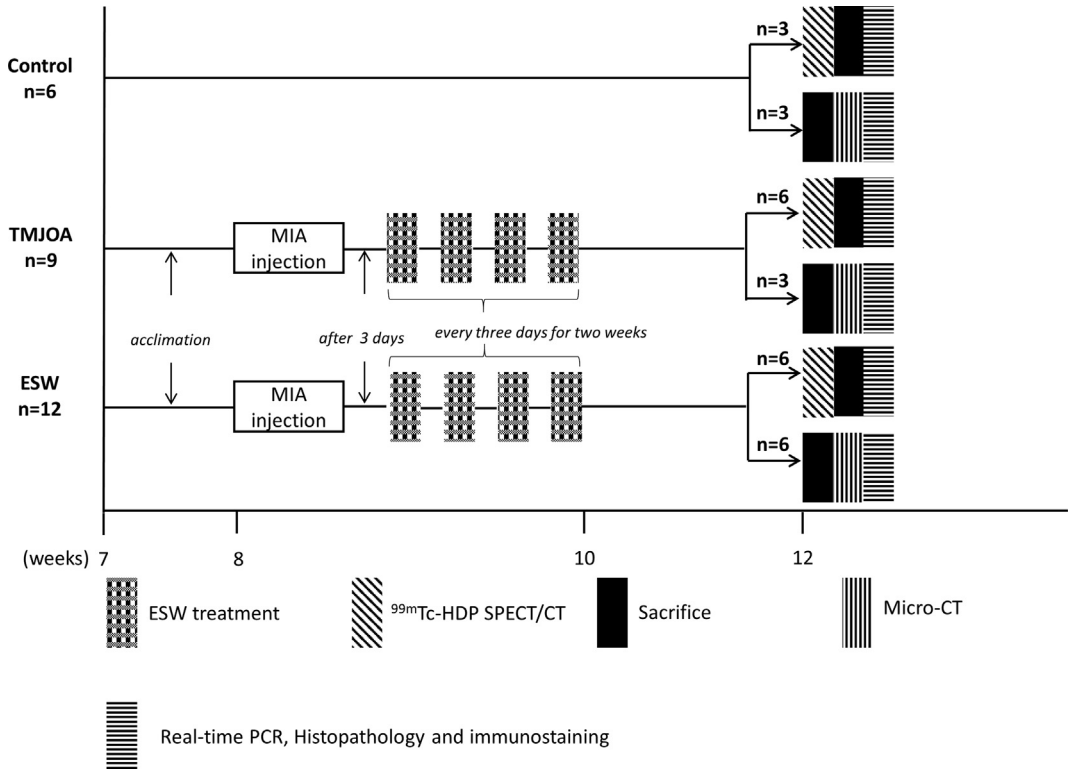

Fig. 3. Experimental schedule for TMJOA rat models and the ESWT application. MIA injection: right TMJ monosodium iodoacetate injection; ESWT: 500 shocks (energy level = 0.068 mJ/mm^2; frequency = 5 pulses/s) to right TMJ every 3 days for 2 weeks, for a total of four treatments.

therapeutic option on TMJ arthritis which were demonstrated on rheumatoid arthritis animal models[26]. From this recent study, pressure waves from LIPUS showed down-regulation of pro-inflammatory cytokine similar to our finding from ESWT.

ESWT has been widely used for different musculoskeletal disorders. Although the exact mechanism of action of ESWT is not known, the clinical success of ESWT is supported by many indirect lines of evidence[27]. ESWT can reduce inflammation and apoptosis while stimulating the regeneration of various tissues[28,29]. For joints, in particular, ESWT has shown a chondroprotective effect[8,12,30,31]. Consistent with previous findings, the current study revealed the effects of ESWT on chondrocytes as seen through the down-regulation of pro-inflammatory cytokine expression (TNF-α, IL-1β, IL-6), apoptosis, and tissue degradation. These effects were confirmed by histological cartilage examinations of rat TMJ.

According to a previous study by Wang *et al.*, thinning of the disc and cartilage does not become apparent until between 4 and 12 weeks, although infiltrated mononuclear cells and loss of chondrocytes in the cartilage of the TMJ disc can be found 3 days after MIA administration[17]. Based on results from our previous study, ESWT might prevent cartilage from thinning by reducing the action of pro-inflammatory cytokines, cartilage degradation, and chondrocyte apoptosis. Considering that ESWT performed prior to MIA treatment on rat chondrocytes was associated with a protective effect therein, ESWT might be a preventive of TMJOA. However, the single time point histological evaluation precludes drawing such a conclusion and is a limitation of our study.

In the current study, the effects of ESWT on TMJ subchondral bone was additionally investigated using ^{99m}Tc-HDP SPECT/CT and micro-CT imaging. Bone scintigraphy, or SPECT, is used for diagnosis of TMJOA and treatment response prediction[32–34]. ^{99m}Tc-HDP SPECT/CT can assess subchondral bone remodeling as a consequence of TMJOA. Although we did not evaluate the biomarkers and histology of the subchondral bone itself, the fact that ^{99m}Tc-HDP uptake ratios were was significantly lower in the ESWT group compared to the TMJOA control group suggests that ESWT does affect the subchondral bones in TMJOA. Also, considering that LIPUS could accelerate the osteoblastic activity[26], ESWT might have an direct effect on subchondral bone itself. This point could be the interesting point in future study of ESWT.

Micro-CT has an extremely high spatial resolution, especially for small objects, and is used to evaluate the microarchitecture of bones in preclinical studies[35]. Classically, OA is characterized by increased subchondral bone sclerosis with thickening of the cortical plate, extensive remodeling of the trabeculae, and the formation of osteophytes, along with progressive loss of articular cartilage[36]. Some studies have shown an increase in bone mineral density and an inverse relationship with osteoporosis in OA[37]. However, other studies have reported that atrophic changes may depend on the location of the involved joints. When individual bones were analyzed, the appendicular skeleton in OA joints showed atrophic changes, especially in the joints of upper extremities[38]. A recent study focused on OA in the condylar bone of the TMJ and reported a decrease in BV/TV in addition to bone loss[39]. In this study, we also found atrophic subchondral bone changes in TMJ, indicating that the relationship between osteoporosis and OA is complex and the pathophysiologic processes of OA are dynamic and differ depending on the joints involved[40].

The interplay between cartilage and subchondral bone is important for OA research. Though we focused on the direct effects of ESWT on TMJ cartilage, changes to subchondral bone induced by ESWT also contributed to beneficial effects on cartilage as the subchondral bone is located just beneath the articular cartilage. However, ESWT-related changes in subchondral bone biomarkers such as type 1 collagen, osteocalcin, or alkaline phosphatase, were not investigated in this study. Based on our ^{99m}Tc-HDP SPECT/CT

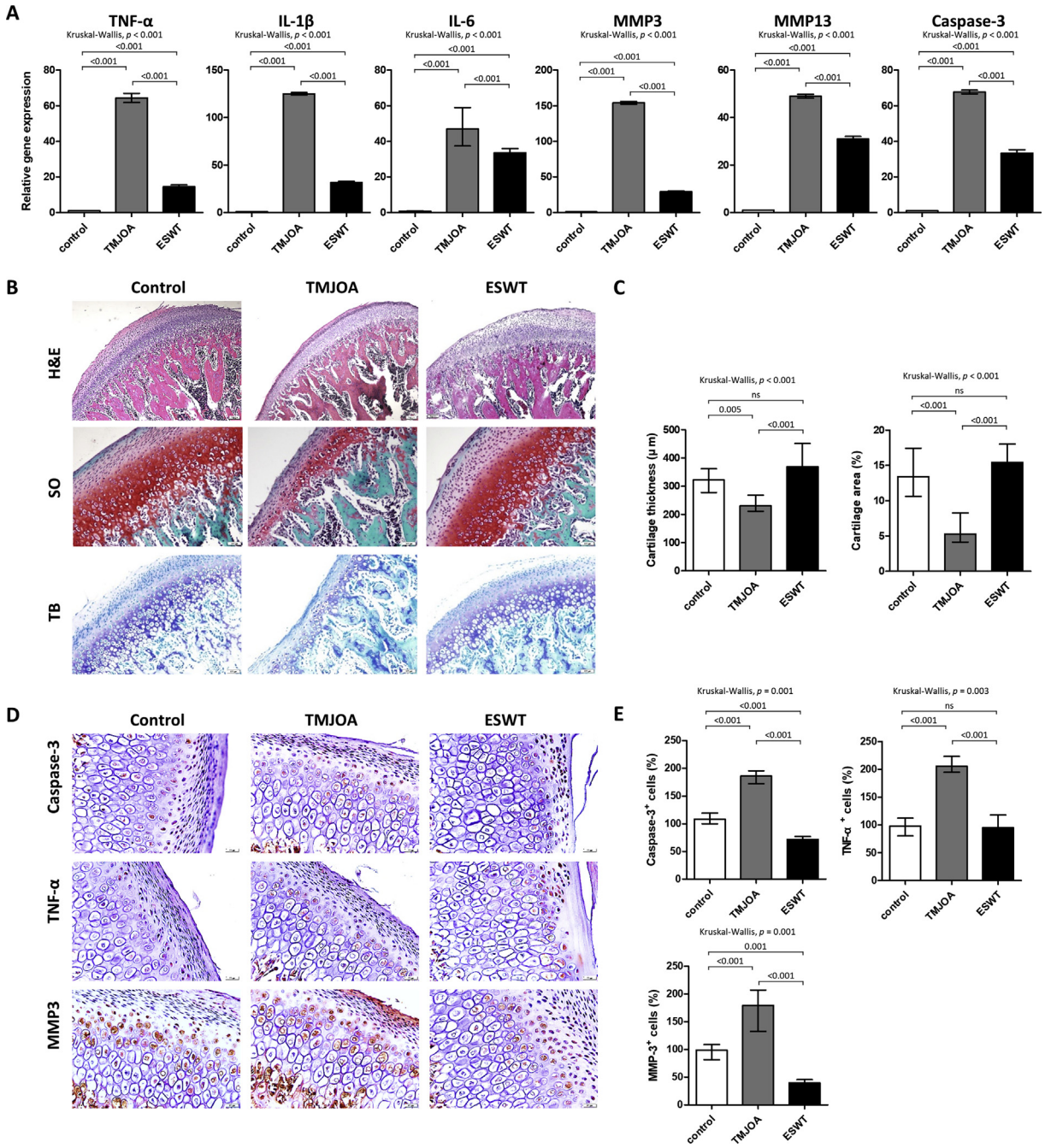

Fig. 4. ***In vivo*** **effects of ESWT on the TMJOA rat model.** Results of PCR, histology, and immunohistochemistry assays on the effects of ESWT (0.068 mJ/mm^2, 5 pulses/s, every 3 days, 4 times in total) on MIA (3.0 μM)-injected TMJ in a rat model (control, $n = 6$; TMJOA, $n = 9$; ESWT, $n = 12$). (A) Real time-PCR expression analysis of TNF-α, IL-1β, IL-6, MMP3, MMP13, and caspase-3 on TMJOA tissues. (B, C) Histopathologic analysis with H&E, safranin O-fast green (SO), and TB. On H&E, TMJOA shows hypocellular changes and thinning of cartilage compared to the control; this was recovered by ESWT. Condylar cartilage was stained red by SO and purple blue by TB. Cartilage thickness and percentage of cartilage area were measured and quantified. (D, E) Immunohistochemical analysis. Representative light microscopic images of caspase-3, TNF-α, and MMP-3 positive chondrocytes in the control and experimental groups. Values are presented median with IQR. Scale bar = 50 μm.

and micro-CT results, future *in vitro* and *in vivo* studies on the protective effects of ESWT on osteoblasts and TMJ subchondral bone are recommended.

Although the exact mechanism of ESWT remains unclear, the alleviation of subchondral bone remodeling might be due to both the mitigation of inflammatory processes in the joints and direct ESW-associated effects on bone architecture[41,42]. Further study on ESWT effects on subchondral bone are necessary, as thus far, only one clinical study has been published on the effects of ESWT on TMDs in humans[13]. Further clinical studies with *in vivo* functional and structural assessments via ^{99m}Tc-HDP SPECT/CT are needed to demonstrate the efficacy of ESWT on TMJOA.

Certain limitations to the current study must be acknowledged. This study was based on a small number of rats, and greater numbers will be necessary before moving on to clinical applications in humans. The use of larger animals could help determine the optimal conditions for ESWT, such as energy levels or shock numbers in preparation for human TMJOA treatment. In addition,

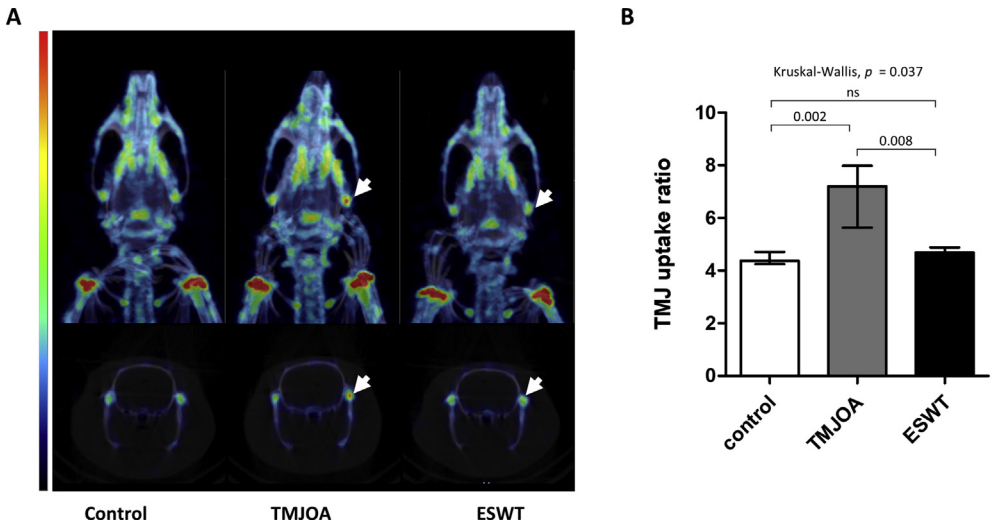

Fig. 5. Representative images of ^{99m}Tc-HDP SPECT/CT of TMJs site (A) and TMJ uptake ratio among three groups (B). (A) 3-dimensional maximal intensity projection (upper raw) and coronal section (lower raw) images of rat TMJ. The control rat shows a symmetrical uptake of bilateral TMJ. For TMJOA, the right TMJ was inflamed with an MIA injection (arrow). For ESWT, the inflamed right TMJ was treated with the head applicator (arrow). (B) TMJ uptake ratios were evaluated and compared among the three groups. Values are presented as median with interquartile range.

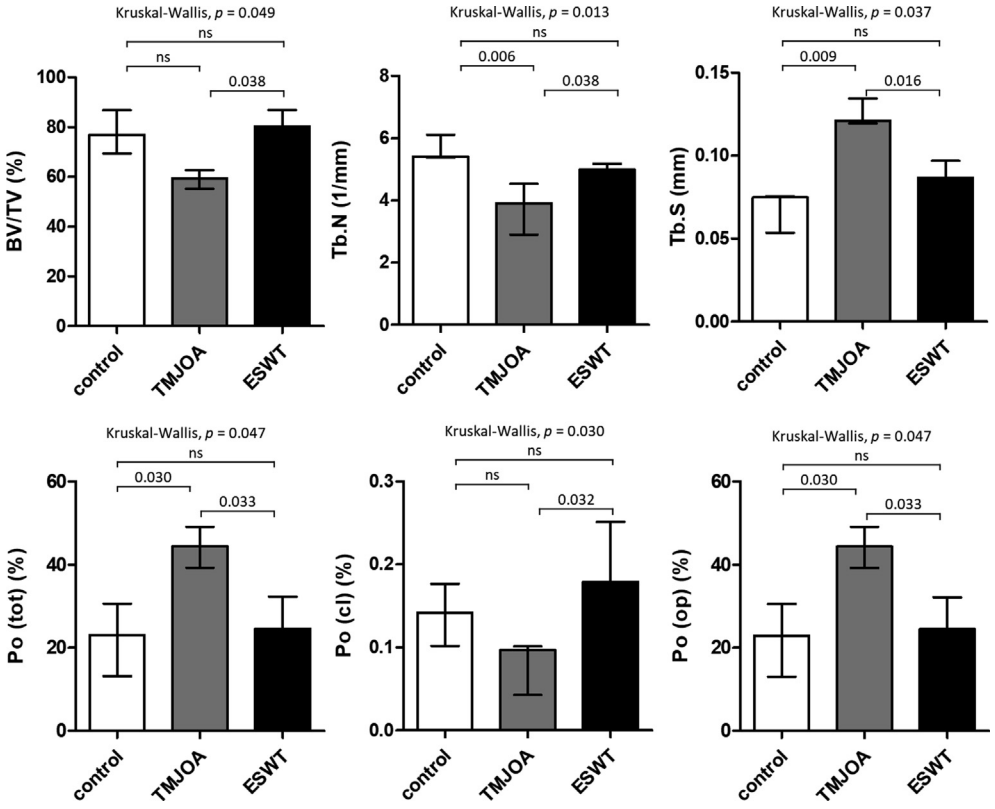

Fig. 6. Results of Micro-CT analysis. Bone volume density (BV/TV), trabecular number (Tb.N), trabecular separation (Tb.S), total porosity (Po(tot)), closed porosity (Po(cl)), and open porosity (Po(op)) were evaluated by micro-CT analysis and compared among the three groups. Values are presented as median with interquartile range.

although ESWT did not damage chondrocyte viability in the current study, considering the anatomy of the TMJ, a complex structure in a narrow area and close to other organs, effects of ESWT on adjacent structures must be evaluated, as well.

In conclusion, ESWT was associated with a protective effect on cartilage and subchondral bone structures of TMJOA in MIA-induced chondrocytes and the MIA TMJOA model in rats. ^{99m}Tc-HDP bone SPECT/CT and micro-CT reflected microenvironmental changes in TMJOA and protective effects related to ESWT. In particular, the uptake of ^{99m}Tc-HDP measured on SPECT/CT may have potential as an imaging biomarker for the effect of ESWT on TMJ.

Author contributions

Conception and design: HJY, BSK.

Acquisition of data: HJS, JHK.

Analysis and interpretation of the data: all authors.

Drafting of the article: JIB, YHJ.

Critical revision of the article for important intellectual content: all authors.

Final approval of the article: all authors.

Conflict of interest

The authors report no conflicts of interests.

Role of the funding source

This research was supported by RP-Grant 2018 of Ewha Womans University (2018-0001-001-1, Bom Sahn Kim) and Basic Science Research Program through the National Research Foundation of Korea (2015R1C1A2A01054113 and 2018R1D1A1B07049400, Hai-Jeon Yoon; 2018R1D1A1B07045321, Bom Sahn Kim; 2018R1D1A1B07045394, Yemi Kim). The funding sources had no role in the study design, data collection or analysis, interpretation of data, writing of the manuscript, or in the decision to submit the manuscript for publication.

Acknowledgments

None.

Supplementary data

Supplementary data to this article can be found online at https://doi.org/10.1016/j.joca.2019.07.008.

References

1. Bansal M. Prevalence and diagnostic features of osteoarthrosis of the temporomandibular joint: a review. Int J Res Orthop 2016;2:1–4.
2. Kalladka M, Quek S, Heir G, Eliav E, Mupparapu M, Viswanath A. Temporomandibular joint osteoarthritis: diagnosis and long-term conservative management: a topic review. J Indian Prosthodont Soc 2014;14:6–15.
3. Wang X, Zhang J, Gan Y, Zhou Y. Current understanding of pathogenesis and treatment of TMJ osteoarthritis. J Dent Res 2015;94:666–73.
4. Vernal R, Velasquez E, Gamonal J, Garcia-Sanz JA, Silva A, Sanz M. Expression of proinflammatory cytokines in osteoarthritis of the temporomandibular joint. Arch Oral Biol 2008;53:910–5.
5. Vos LM, Kuijer R, Huddleston Slater JJ, Bulstra SK, Stegenga B. Inflammation is more distinct in temporomandibular joint osteoarthritis compared to the knee joint. J Oral Maxillofac Surg 2014;72:35–40.
6. Wang X, Cui S, Liu Y, Luo Q, Du R, Kou X, *et al*. Deterioration of mechanical properties of discs in chronically inflamed TMJ 2014;93:1170–6.
7. Tanaka E, Detamore MS, Mercuri LG. Degenerative disorders of the temporomandibular joint: etiology, diagnosis, and treatment. J Dent Res 2008;87:296–307.
8. Wang CJ, Sun YC, Wong T, Hsu SL, Chou WY, Chang HW. Extracorporeal shockwave therapy shows time-dependent chondroprotective effects in osteoarthritis of the knee in rats. J Surg Res 2012;178:196–205.
9. Wang CJ. Extracorporeal shockwave therapy in musculoskeletal disorders. J Orthop Surg Res 2012;7:11.
10. Mariotto S, Cavalieri E, Amelio E, Ciampa AR, de Prati AC, Marlinghaus E, *et al*. Extracorporeal shock waves: from lithotripsy to anti-inflammatory action by NO production. Nitric Oxide 2005;12:89–96.
11. Sofia M, Alessandra Carcereri de P, Elisabetta C, Ernesto A, Ernst M, Hisanori S. Extracorporeal shock wave therapy in inflammatory diseases: molecular mechanism that triggers anti-inflammatory action. Curr Med Chem 2009;16:2366–72.
12. Zhao Z, Ji H, Jing R, Liu C, Wang M, Zhai L, *et al*. Extracorporeal shock-wave therapy reduces progression of knee osteoarthritis in rabbits by reducing nitric oxide level and chondrocyte apoptosis 2012;132:1547–53.
13. Yin C, Xia W, Zhang X, Zheng C, Ren S. Extracorporeal shock wave therapy for treating disorders of the temporomandibular joint. Chin J Phys Med Rehabil 2016;38:425–8.
14. Jiang L, Li L, Geng C, Gong D, Jiang L, Ishikawa N, *et al*. Monosodium iodoacetate induces apoptosis via the mitochondrial pathway involving ROS production and caspase activation in rat chondrocytes in vitro. J Orthop Res 2013;31:364–9.
15. Canaparo R, Serpe L, Catalano MG, Bosco O, Zara GP, Berta L, *et al*. High energy shock waves (HESW) for sonodynamic therapy: effects on HT-29 human colon cancer cells. Anticancer Res 2006;26:3337–42.
16. Ogata K, Katagiri W, Osugi M, Kawai T, Sugimura Y, Hibi H, *et al*. Evaluation of the therapeutic effects of conditioned media from mesenchymal stem cells in a rat bisphosphonate-related osteonecrosis of the jaw-like model. Bone 2015;74:95–105.
17. Wang XD, Kou XX, He DQ, Zeng MM, Meng Z, Bi RY, *et al*. Progression of cartilage degradation, bone resorption and pain in rat temporomandibular joint osteoarthritis induced by injection of iodoacetate. PLoS One 2012;7:e45036.
18. Schmitz N, Laverty S, Kraus VB, Aigner T. Basic methods in histopathology of joint tissues. Osteoarthritis Cartilage 2010;18(Suppl 3):S113–6.
19. Jiao K, Zeng G, Niu L-N, Yang H-x, Ren G-t, Xu X-y, *et al*. Activation of α2A-adrenergic signal transduction in chondrocytes promotes degenerative remodelling of temporomandibular joint. Sci Rep 2016;6:30085.
20. Sun Yoo J, Lee J, Ho Jung J, Seok Moon B, Kim S, Chul Lee B, *et al*. SPECT/CT imaging of high-risk atherosclerotic plaques using integrin-binding RGD dimer peptides. Sci Rep 2015;5:11752.
21. microCT B, Ed. Analysis of Bone by Micro-CT General Information 2013:1–41.
22. Becker M, Souza MA, Moraes LG, Silva GS, Antoniassi NA, Souza RL, *et al*. Bone quality evaluation of experimental osteometabolic disease in Pantanal alligators (Caiman yacare) by High Resolution Computerized Microtomography (μCT). Pesqui Vet Bras 2018;38:981–90.
23. Cevidanes LH, Walker D, Schilling J, Sugai J, Giannobile W, Paniagua B, *et al*. 3D osteoarthritic changes in TMJ condylar morphology correlates with specific systemic and local biomarkers of disease. Osteoarthritis Cartilage 2014;22:1657–67.
24. Su S-C, Tanimoto K, Tanne Y, Kunimatsu R, Hirose N, Mitsuyoshi T, *et al*. Celecoxib exerts protective effects on extracellular matrix metabolism of mandibular condylar chondrocytes under excessive mechanical stress. Osteoarthritis Cartilage 2014;22:845–51.
25. Chen K, Man C, Zhang B, Hu J, Zhu SS. Effect of in vitro chondrogenic differentiation of autologous mesenchymal stem cells on cartilage and subchondral cancellous bone repair in osteoarthritis of temporomandibular joint. Int J Oral Maxillofac Surg 2013;42:240–8.
26. Crossman J, Alzaheri N, Abdallah M-N, Tamimi F, Flood P, Alhadainy H, *et al*. Low intensity pulsed ultrasound increases

mandibular height and Col-II and VEGF expression in arthritic mice. Arch Oral Biol 2019;104:112–8.
27. Moya D, Ramón S, Schaden W, Wang C-J, Guiloff L, Cheng J-H. The role of extracorporeal shockwave treatment in musculoskeletal disorders. JBJS 2018;100:251–63.
28. Chen Y-L, Chen K-H, Yin T-C, Huang T-H, Yuen C-M, Chung S-Y, *et al*. Extracorporeal shock wave therapy effectively prevented diabetic neuropathy. Am J Transl Res 2015;7:2543–60.
29. Ciampa AR, de Prati AC, Amelio E, Cavalieri E, Persichini T, Colasanti M, *et al*. Nitric oxide mediates anti-inflammatory action of extracorporeal shock waves. FEBS Lett 2005;579:6839–45.
30. Wang CJ, Hsu SL, Weng LH, Sun YC, Wang FS. Extracorporeal shockwave therapy shows a number of treatment related chondroprotective effect in osteoarthritis of the knee in rats. BMC Musculoskelet Disord 2013;14:44.
31. Wang C-J, Weng L-H, Ko J-Y, Sun Y-C, Yang Y-J, Wang F-S. Extracorporeal shockwave therapy shows chondroprotective effects in osteoarthritic rat knee. Arch Orthop Trauma Surg 2011;131:1153–8.
32. Katzberg RW, O'Mara RE, Tallents RH, Weber DA. Radionuclide skeletal imaging and single photon emission computed tomography in suspected internal derangements of the temporomandibular joint. J Oral Maxillofac Surg 1984;42:782–7.
33. Lee SM, Lee WW, Yun PY, Kim YK, Kim SE. Prediction of splint therapy efficacy using bone scan in patients with unilateral temporomandibular disorder. Nucl Med Mol Imaging 2009;43:143–9.
34. Suh MS, Lee WW, Kim Y-K, Yun P-Y, Kim SE. Maximum standardized uptake value of 99mTc hydroxymethylene diphosphonate SPECT/CT for the evaluation of temporomandibular joint disorder. Radiology 2016;280:890–6.
35. Faot F, Chatterjee M, de Camargos GV, Duyck J, Vandamme K. Micro-CT analysis of the rodent jaw bone micro-architecture: a systematic review. Bone Reports 2015;2:14–24.
36. Sharma A, Jagga S, Lee S-S, Nam J-S. Interplay between cartilage and subchondral bone contributing to pathogenesis of osteoarthritis. Int J Mol Sci 2013;14:19805–30.
37. Hart DJ, Mootoosamy I, Doyle DV, Spector TD. The relationship between osteoarthritis and osteoporosis in the general population: the Chingford Study. Ann Rheum Dis 1994;53:158–62.
38. Im GI, Kim MK. The relationship between osteoarthritis and osteoporosis. J Bone Miner Metab 2014;32:101–9.
39. Shi J, Lee S, Pan H, Mohammad A, Lin A, Guo W, *et al*. Association of condylar bone quality with TMJ osteoarthritis. J Dent Res 2017;96:888–94.
40. Felson DT, Nevitt MC. Epidemiologic studies for osteoarthritis: new versus conventional study design approaches. Rheum Dis Clin North Am 2004;30:783–97. vii.
41. Haupt G, Haupt A, Ekkernkamp A, Gerety B, Chvapil M. Influence of shock waves on fracture healing. Urology 1992;39:529–32.
42. Lai JP, Wang FS, Hung CM, Wang CJ, Huang CJ, Kuo YR. Extracorporeal shock wave accelerates consolidation in distraction osteogenesis of the rat mandible. J Trauma 2010;69:1252–8.